

Electronic Supplementary Information

“Proof-of-principle” concept for ultrasensitive detection of cytokine based on the electrically heated carbon paste electrode

Jing-Jing Zhang, Yan Liu, Li-Hui Hu, Li-Ping Jiang* and Jun-Jie Zhu*

*Key Lab of Analytical Chemistry for Life Science (MOE), School of Chemistry and Chemical
Engineering, Nanjing University, Nanjing, 210093, P.R. China*

Experimental

Materials. Multi-walled carbon nanotubes (CNTs, CVD method, purity >95%, diameter 10-20 nm, length 0.5-2.0 μm) were purchased from Nanoport. Co. Ltd. (Shenzhen, China). Poly(diallyldimethylammonium chloride) (PDDA, 20%, w/w, in water, MW= 200,000–350,000), 1-ethyl-3-(3-dimethylaminopropyl) carbodiimide hydrochloride (EDC), N-hydroxysuccinimide (NHS), 2-(N-morpholino)ethanesulfonic acid (MES), 3-mercaptopropionic acid (MPA), Bovine serum albumin (BSA, 96–99%), and Dopamine (DA) were from Sigma-Aldrich (St. Louis, USA). Human Interleukin-6 (IL-6), Human Interleukin-6 ELISA Kit, Polyclonal anti-IL-6, Carcinoembryonic antigen (CEA), C-reactive protein (CRP), and Tumor Necrosis Factor-Alpha (TNF- α) were obtained from Beijing Biosynthesis Biotechnology Co. Ltd. (Beijing, China). The serum sample from leukemia patients were obtained anonymously from Nanjing Gulou Hospital and used as received. When the levels of analyte were over the detection dynamic ranges, serum samples were appropriately diluted with 0.01 M PBS (pH 7.4) prior to the assay. Carbon ink and silver ink were obtained from Camnano Technology Company, Ltd. (Xuzhou, China). $\text{HAuCl}_4 \cdot 4\text{H}_2\text{O}$ ($\text{Au}\% >$

48%) was from Shanghai Chemical Reagent Co. (Shanghai, China). Phosphate buffer saline (PBS, 0.01 M, pH 7.4) contained 136.7 mM NaCl, 2.7 mM KCl, 8.7 mM Na₂HPO₄ and 1.4 mM KH₂PO₄. All other reagents were of analytical grade. All aqueous solutions were prepared using ultra-pure water (Milli-Q, Millipore).

The PDDA-functionalized graphene (PDDA-RGO) was prepared as reported previously.¹ The obtained PDDA-RGO was redispersed in water to a concentration of 1.0 mg mL⁻¹.

Preparation of RGO-AuNPs nanocomposite. The RGO-AuNPs was prepared by two-step assembly process, as depicted in Fig. 1A., First, the polydopamine-stabilized gold nanoparticles (PDA-AuNPs) were chemically synthesized according to the literature with slightly modification.² Briefly, reductive dopamine solution was quickly mixed with oxidative HAuCl₄ solution (2 wt%), and the final concentration of DA and HAuCl₄ were 20.0 mM and 10.0 mM, respectively. The mixture was incubated at 4 °C for 1h and centrifuged at 5 000 rpm for 5 min. The PDA-AuNPs could be obtained after discarding the sediment. Subsequently, 100 μL of 1.0 mg mL⁻¹ PDDA-RGO was added into 1.0 mL of freshly prepared PDA-AuNPs, and the resulting dispersion was sonicated for 60 min to give a homogeneous black suspension. The reaction mixture was centrifuged at 18 000 rpm for 10 min and washed with PBS for three times, and the supernatant was discarded. The obtained RGO-AuNPs was redispersed in 1.0 mL of pH 7.4 PBS and stored at 4 °C. The final concentration of PDA-AuNPs was controlled as 1.0 mg mL⁻¹.

Synthesis of MPA-capped CdTe QDs. The MPA-capped CdTe QDs were prepared as reported previously.³ Briefly, 0.1142 g of CdCl₂•2.5H₂O and 0.0849 g of MPA were successively dissolved in 198 mL of ultra-pure water under N₂ atmosphere, and the pH was adjusted to 8.0-8.5 by the addition of a 5% NaOH solution. Subsequently, 2.0 mL of freshly prepared NaHTe solution produced by the reaction of KBH₄ (0.0480 g, 0.89 mM) with tellurium powder (0.0480 g, 0.375 mM) in a 2.0 mL

aqueous solution was mixed with above CdCl₂-MPA solution. The reactant mixture was then refluxed under N₂ atmosphere at about 96 °C for 3h to obtain a red CdTe QDs solution.

Preparation of CNTs@QDs-anti-IL-6 bionanoplabel. The CNTs@QDs-anti-IL-6 bionanoplabel was prepared via a layer-by-layer (LbL) assembly approach. Briefly, 50.0 mg of CNTs was dispersed in a mixture of sulfuric acid and nitric acid (3:1) and sonicated for 3 h to obtain carboxylic group-functionalized CNTs. After centrifugation from the mixture, the sediment was washed repeatedly with water until the pH reached 7.0. Then, 10.0 mg of oxidized CNTs was dispersed into a 0.5 wt% PDDA salt solution (0.5M NaCl, 10 mL) and the resulting dispersion was sonicated for 60 min to give a homogeneous black suspension. Residual PDDA polymer was removed by high-speed centrifugation (20, 000 rpm, 15 min) at room temperature and the complex was rinsed with water for at least three times. Subsequently, 3.0 mL of CdTe QDs solution was added into a 2 mL dispersion of PDDA functionalized CNTs (2.5 mg mL⁻¹) and the reaction mixture was sonicated for 60 min. Excess particles were removed by subsequent centrifugation and redispersion in water. This procedure resulted in homogeneous coating of the CNTs surface with QDs, and the CNTs@CdTe QDs composite solution was obtained. Finally, 1.0 mL of CNTs@QDs (2.0 mg mL⁻¹) was mixed with 3.2 mg of EDC and 0.1 mg of anti-IL-6 in 50 mM pH 5.2 MES buffer, and incubated 2 h at room temperature under shaking and kept overnight at 4 °C. The reaction mixture was washed with PBS and centrifuged at 13 000 rpm for 5 min three times, and the supernatant was discarded. The obtained CNTs@QDs-anti-IL-6 bionanoplabel was redispersed in 1.0 mL of pH 7.4 PBS containing 3% BSA and stored at 4 °C. The final concentration of the bionanoplabel was controlled as 1.0 mg mL⁻¹.

Construction of Electrically Heated Carbon Paste electrode (HCPE). The structure of a HCPE is sketched in Fig. S1. On 0.5-mm-thick glass fiber plate as the substrate material, the heated carbon

paste working electrode (planar area: 10 mm × 2 mm) was firstly fabricated from carbon ink. Silver ink, acting as conductive medium, was printed as the second layer. The insulating ink (Jelcon AC-3G, Jujo Chemical Company, Ltd., Japan) was used to provide the insulation layer, defining a thin-layer electrochemical micro-cell. The three carbon ink strips served as the electrical contacts. The central contact (Fig. S1A) provides the connection to the electrochemical workstation, with the other two (Fig. S1B) connected to the heating device (possess about 120 Ω resistance). The HCPE needed vacuum drying at 100 °C for 30 min after each step of the printing process. Finally, the HCPE was vacuum dried at 140 °C for 90 min. Before use, the HCPE was cleaned by washing with PBS and dried at room temperature. The prepared HCPE was facile, low cost and disposable, which had potential application in clinic chemistry.

Construction of Electrically Heated detection system. The Electrically Heated detection system equipped with an electrically heated CPE is shown schematically in Fig. S2. The overall setup consists of a HCPE working system, electrochemical detection unit and a heating device. The heating current (100 kHz ac) was provided by a function generator (DF1027B, Ningbo Zhongce Electronics Co., Ltd., China) with 40 W peak power. The output was connected to the electrode via a transformer. The heating current was monitored by measuring the voltage drop of 1 Ω resistance serially connected to the electrode with an alternating current (ac) millivolt meter (DF1933, Ningbo Zhongce Electronics Co., Ltd., China).

Fabrication of the electrochemical immunosensor. The heated-electrode immunoassay protocol was shown in Fig. 1C. 10.0 μL of 1.0 mg mL⁻¹ RGO-AuNPs solution was first dropped on the electrode and dried in a silica gel desiccator. After being thoroughly rinsed with deionized water, the modified electrode was immediately incubated in 5.0 μL of 100 μg mL⁻¹ IL-6 solution at 4 °C for at least 24 h in a moisture atmosphere to avoid evaporation of solvent, following a carefully rinse with

0.1 M pH 7.4 PBS to remove physically absorbed protein. After that, the electrode was immersed in 100 μL of 10.0 mg mL^{-1} BSA solution at 37 $^{\circ}\text{C}$ for 1 h to block the active sites of the electrode. Then the electrode was taken out, and carefully rinsed with pH 7.4 PBS and dried at room temperature. Subsequently, 10.0 μL of incubation solution, which was prepared by mixing 5.0 μL of IL-6 sample or real serum sample with 5.0 μL of 1.0 mg mL^{-1} CNTs@QDs-anti-IL-6 bionanoparticle, was carefully dropped on the electrode and incubated at 37 $^{\circ}\text{C}$ under saturation humidity for 40 min. Finally, the electrode was washed thoroughly with pH 7.4 PBS to remove non-specifically bound conjugates to minimize the background response.

Electrochemical detection of captured QDs-based bionanoparticle. After the binding, the electrode was immersed in 200 μL of 0.1 M HNO_3 solution for 2 h to dissolve the captured QDs, and the resulting solution was mixed with 0.8 mL of 0.2 M pH 4.6 HAc-NaAc buffer containing 10.0 $\mu\text{g mL}^{-1}$ Bi^{2+} to perform anodic stripping voltammetric detection with a conventional three-electrode system comprised of platinum wire as auxiliary electrode, saturated calomel electrode (SCE) as reference, and a heated electrode (HCPE) as working electrode. The anodic stripping detection was carried out by depositing cadmium at -1.1 V for 400 s and then stripping from -1.0 V to -0.5 V using a square-wave voltammetric waveform, with a 4 mV potential step, a 25 Hz frequency, and an amplitude of 25 mV. In the case of deposition at heated electrode, the alternating heating current was applied only during the accumulation period, and turned off 10 s prior to the stripping step. The electrode temperature was controlled at 49.0 $^{\circ}\text{C}$. For comparison, the same detection procedure was also carried out by unheated electrode (CPE) at room temperature about 25.0 $^{\circ}\text{C}$.

General Procedure of ELISA Assay. An IL-6 standard was supplied with the Human IL-6 Sandwich ELISA Kit. A standard curve for the spectrophotometric procedure was produced by following the manufacturer's protocol with a range of detection between 0 and 500 pg mL^{-1} .

Concentrations of IL-6 in serum sample were detected spectrophotometrically by measuring absorbance changes at 450 nm. Briefly, the serum sample or IL-6 standard (0–500 pg mL⁻¹) were added to the ELISA plate (50 µL/well) and incubated 1 h at 37 °C. Then each well of the plate was washed five times with 200 µL of wash buffer. Enzyme-labeled bioconjugation solution was added to each well and incubated for 30 min at 37 °C and washed again with wash buffer. Subsequently, substrate solution (50 µL solution A and 50 µL solution B) was added to each well and incubated 15 min in the dark. Without washing the plate, 50 µL of stop solution was added to each well to stop the color reaction. The absorbance was read immediately on an automated plate reader (model 680, Bio-RAD) at 450 nm.

Apparatus. Transmission electron micrographs (TEM) were measured on a JEOLJEM 200CX transmission electron microscope, using an accelerating voltage of 200 kV. UV-vis spectra were recorded on a UV-3600 spectrophotometer (Shimadzu, Kyoto, Japan). X-ray powder diffraction (XRD) measurements were performed on a Japan Shimadzu XRD-6000 Diffractometer with Cu K α radiation ($\lambda=0.15418$ nm); a scanning rate of 0.05 deg/s was applied to record the patterns in the 2θ range of 20–80°. Electrochemical measurements were performed on a CHI 660B workstation (Shanghai Chenhua Apparatus Corporation, China) with a conventional three-electrode system comprised of a platinum wire as the auxiliary, a saturated calomel electrode as the reference, and the modified HCPE as the working electrode. Electrochemical impedance spectroscopy (EIS) was performed with an Autolab electrochemical analyzer (Eco Chemie, The Netherlands) in a 10 mM K₃Fe(CN)₆/K₄Fe(CN)₆ (1:1) mixture with 1.0 M KCl as the supporting electrolyte, using an alternating current voltage of 5.0 mV, within the frequency range of 0.1 Hz–10 kHz. The static water contact angles were measured at 25 °C by a contact angle meter (Rame-Hart-100) employing drops of pure deionized water. The readings were stabilized and taken within 120 s after the addition.

Design and construction of the heated-electrode system

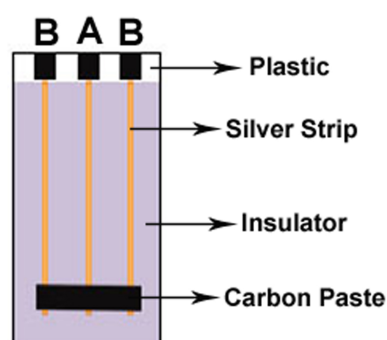


Fig. S1. Scheme of the HCPE: (A) working electrode contact (B) connection to ac heating device.

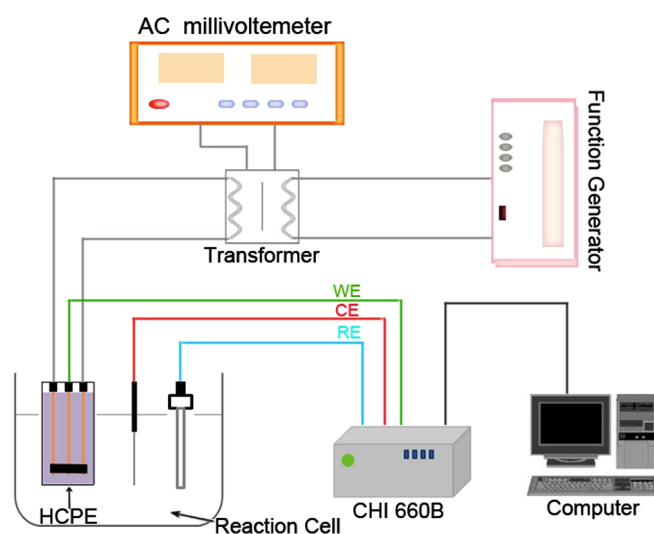


Fig. S2. Schematic diagram of the immunosensor detection system equipped with an electrically heating HCPE. WE: working electrode; RE: reference electrode; CE: counter electrode.

Characterization of the heated-electrode system

The corresponding temperature of the HCPE was measured according to the reports,⁴ on the basis of the well-known temperature coefficient of the ferro/ferricyanide couple. The standard potential of this couple shifted about 1.56 mV K^{-1} in the negative direction. Measurements of the open circuit potential of this reversible redox couple during heating resulted in a linear relation between the square of the heating current and temperature, which indicated that the electrode temperature could be adjusted arbitrarily in a reproducible manner. A good linearity was obtained with a regression coefficient of about 0.99 in the range between 0 and $32.5 \text{ }^\circ\text{C}$ as shown in Figure S3.

The ferri/ferrocyanide redox couple was further used to evaluate the electrochemical performance of the proposed heated-electrode detection system. As shown in Fig. S3B, with successive increases of the electrode temperature, the currents were remarkably increased due to the enhanced convective transport, implying that the enhanced electrochemical signals could be gained at elevated temperature.

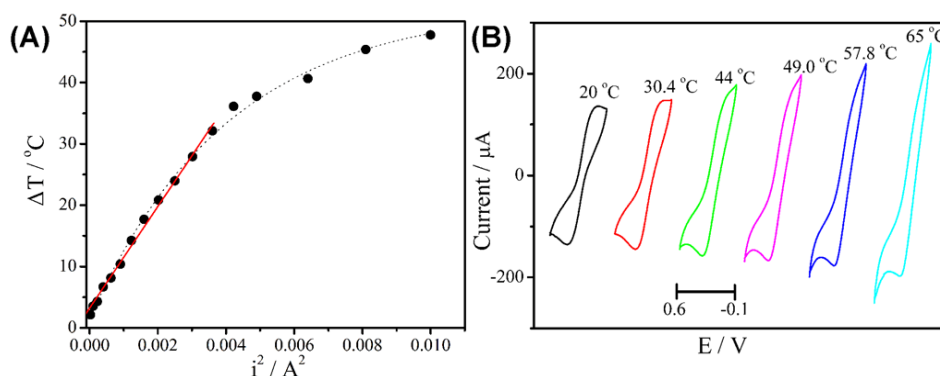


Fig. S3. (A) Dependence of the temperature increase at bare HCPE on the square of heating currents. (B) Cyclic voltammograms of bare HCPE in 0.5 M KCl solution containing 5.0 mM $\text{Fe}(\text{CN})_6^{3-/4-}$ at different temperatures. Scan rate: 100 mV s^{-1} .

The effect of HCPE signal enhancement in the detection of metal ions was also investigated. As shown in Fig. S4, the stripping peak currents for Cd^{2+} increase clearly with increasing the electrode temperature from 26.7 to 57.8 °C. However, when the electrode temperature was more than 60 °C, the temperature rise (ΔT) on our designed HCPE was not linearly with the square of heating current (see Fig. S3A). In that case, the real electrode temperature could not be deduced based on the linear temperature dependence of the equilibrium electrode potential of a reversible redox couple. As a proof of principle study, we chose 49.0 °C to demonstrate the ability of the heated electrode technique to improve the sensitivity of immunosensor.

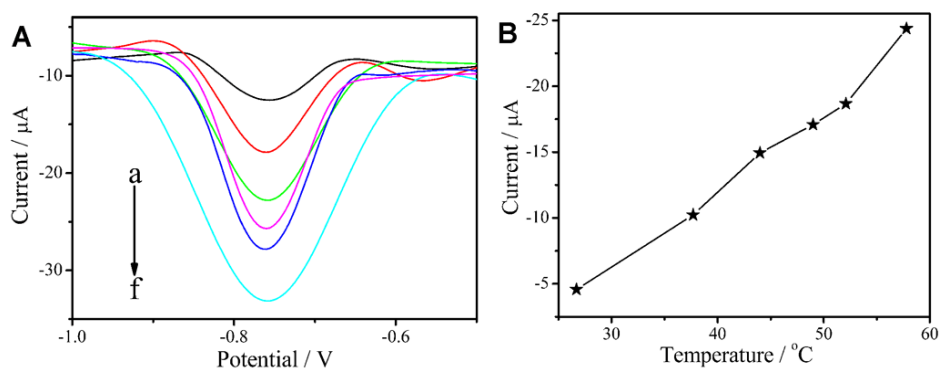


Fig. S4. (A) Anodic stripping voltammograms recorded in 1.0 mL 0.1 M acetate buffer (pH 4.5) containing $5.0 \mu\text{g mL}^{-1}$ Cd^{2+} and $10.0 \mu\text{g mL}^{-1}$ Bi^{2+} on HCPE at different electrode temperatures: (a) 26.7°C , (b) 37.7°C , (c) 44.0°C , (d) 49.0°C , (e) 52.1°C , and (f) 57.8°C . (B) Plot for the dependence of peak currents on the electrode temperature.

Static Contact Angle Measurement

The hydrophilicity of an electrode surface is commonly used to characterize its biocompatibility, which could be measured with the contact angle of the substrate. As shown in Figure S5, the contact angles of the bare glass carbon electrode (GCE), RGO, PDDA-RGO and RGO-AuNPs were $86.5 \pm 0.1^\circ$, $76.9 \pm 1.7^\circ$, $34.3 \pm 1.1^\circ$, and $19.0 \pm 0.3^\circ$, respectively. The RGO-AuNPs film showed the lowest contact angle, indicating better hydrophilicity, which might be attributed to the assembly of PDA-AuNPs on the surface of PDDA-AuNPs. This could introduce a large number of hydrophilic groups, such as hydroxyl group. Thus, the improved biocompatibility of RGO-AuNPs nanocomposite film was in favor of enhancing protein loading and retaining the bioactivity, which thus improves the sensitivity of the immunosensor.

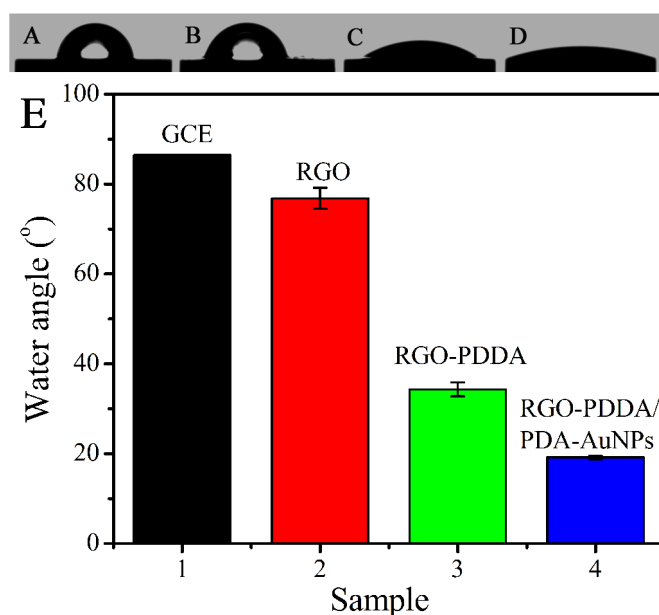


Fig. S5. Contact angle of bare GCE (A), RGO/GCE (B), PDDA-RGO/GCE (C), and RGO-AuNPs/GCE (D). (E) The corresponding histogram.

Characterization of the CNTs-QDs composite.

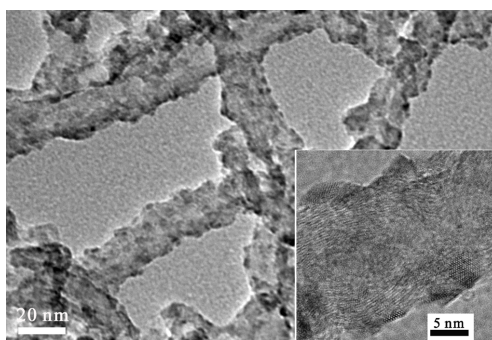


Fig. S6. TEM image of CNTs@QDs nanocomposite. Inset: high magnification of the CNTs surface, illustrating the uniformity of the coating and the presence of the CdTe nanocrystals.

Electrochemical characteristics of the stepwise modified electrodes

Electrochemical impedance spectroscopy (EIS) can give further information on the impedance changes of the immunosensor surface in the modification process. As shown in Fig. S7, compared with the bare GCE (a), the EIS of RGO-AuNPs/GCE showed a lower resistance (b), implying that RGO-AuNPs was an excellent electric conducting material and accelerated electron transfer. Then, the immobilization of IL-6 generated an insulating protein layer, which increased the resistance (c),

confirming that the immunosensor was fabricated. Finally, the increased EIS after BSA blocking indicated that BSA has blocked the free sites on the sensor surface (d), leaving only the available recognition sites for antigen binding.

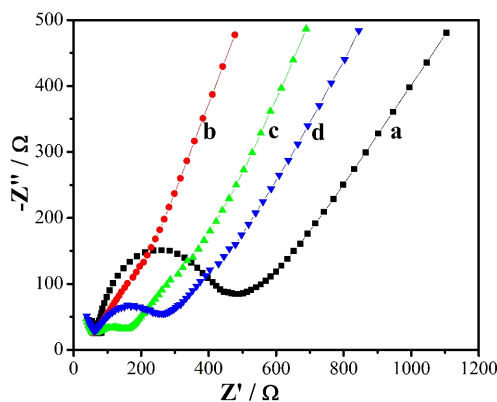


Fig. S7. EIS of (a) GCE, (b) RGO-AuNPs/GCE, (c) IL-6/RGO-AuNPs/GCE, and (d) BSA/IL-6/RGO-AuNPs/GCE in 10.0 mM $[\text{Fe}(\text{CN})_6]^{3-/4-}$ containing 1.0 M KCl.

Optimization of experimental conditions

To obtain high analytical performance, some important detection parameters were optimized (Fig. S8). With the increasing concentration of QDs nanoprobe, the peak current sharply increased and tended to a steady value after 1.0 mg mL^{-1} , indicating that all the available recognition sites of immobilized IL-6 were matched with the nanoprobe (Fig. S8A). Thus, 1.0 mg mL^{-1} was chosen as the optimal nanoprobe concentration. Furthermore, at the optimized nanoprobe concentration, with the incubation time increasing from 5 to 50 min, the immunosensor showed an increasing response until an incubation time of 40 min (Fig. S8B). For sufficient recognition of target protein, 40 min was chosen as the optimal incubation time.

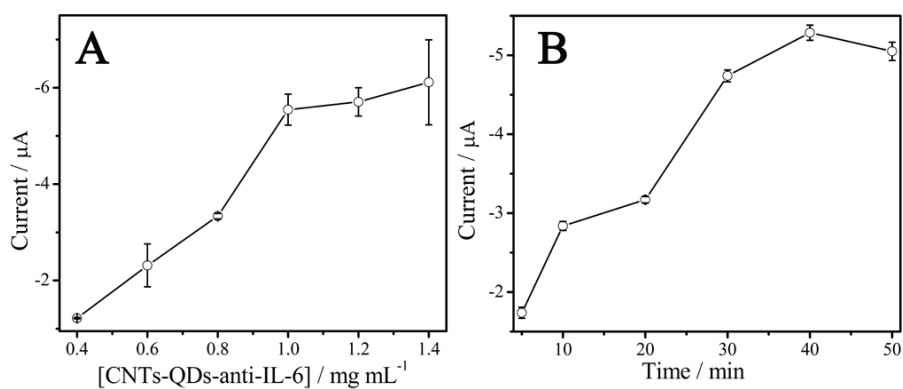


Fig. S8. Effects of CNTs@QDs-anti-IL-6 concentration (A) and incubation time (B) on peak currents of ASV on HCPE for 100 pg mL⁻¹ IL-6.

Linear performance of the immunosensor

For electrochemical detection on HCPE at 49.0 °C, it is found that the decrease of peak current (Δi_p) has a linear dependence on the logarithmic concentration of IL-6 (c) in the range of 0.1-100 pg mL⁻¹. The linear regression equation was $\Delta i_p = 7.78 + 7.65 \times \text{Log } c$, with the linear regression coefficient $R = 0.984$. Correspondingly, the linear response range was only 1.0-10 pg mL⁻¹ on CPE at room temperature. The linear regression equation was $\Delta i_p = 1.63 + 4.65 \times \text{Log } c$, with the linear regression coefficient $R = 0.999$. Obviously, the sensitivity could be improved by using HCPE at high temperature.

Selectivity, reproducibility, and stability

In order to assess the possibility of interference, Carcinoembryonic antigen (CEA), C-reactive protein (CRP), Tumor necrosis factor-alpha (TNF- α), and Bovine Serum Albumin (BSA) were selected to study the specificity (Fig. S9A). Comparing with the current responses to IL-6, all the responses to four interferences each at a 10-fold concentration of IL-6 were neglectable. Thus, the response of the present method was very selective for IL-6. The proposed immunosensor also showed good reproducibility with relative standard deviations of 4.1% and 4.4% at IL-6 concentrations of 10 and 100 pg mL⁻¹ for five independently measurements. When the

immunosensor was not in use, it was stored at 4 °C. More than 90 % of the initial response of the immunosensor for IL-6 remained after one week (Fig. S9B), indicating acceptable stability.

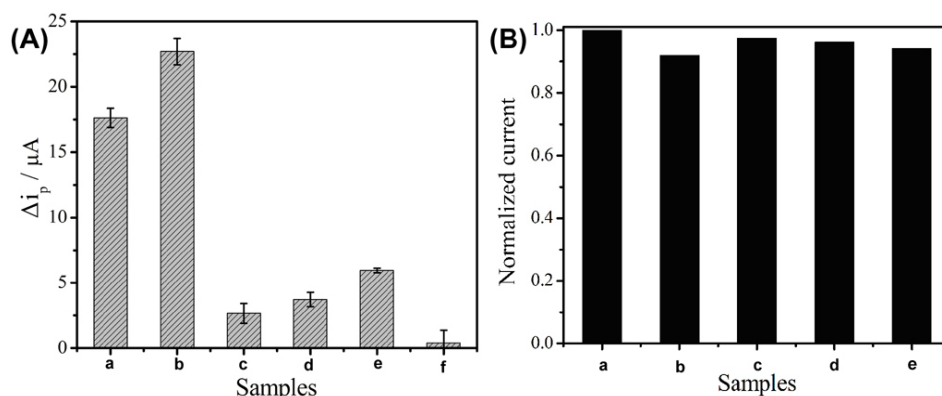


Fig. S9. (A) The specificity of the immunosensor towards other proteins. The decrease of peak currents (Δi_p) to (a) 10 pg mL^{-1} IL-6, (b) 100 pg mL^{-1} IL-6, (c) 100 pg mL^{-1} CEA, (d) 100 pg mL^{-1} CRP, (e) 100 pg mL^{-1} TNF- α , and 100 pg mL^{-1} BSA. (B) Normalized currents of the immunosensor for 100 pg mL^{-1} IL-6 after 7 d storage: (a) control, (b)-(e) 7 d.

References

1. K. P. Liu, J. J. Zhang, G. H. Yang, C. M. Wang, J. J. Zhu, *Electrochem. Commun.*, 2010, **12**, 402–405.
2. Y. C. Fu, P. H. Li, T. Wang, L. J. Bu, Q. J. Xie, X. H. Xu, L. H. Lei, C. Zou, J. H. Chen, S. Z. Yao, *Biosens. Bioelectron.*, 2009, **25**, 1699–1704.
3. R. J. Cui, H. C. Pan, J. J. Zhu, H. Y. Chen, *Anal. Chem.*, 2007, **79**, 8494–8501.
4. Z. Z. Yin, J. J. Zhang, L. P. Jiang, J. J. Zhu, *J. Phys. Chem. C* 2009, **113**, 16104–16109.